JOURNAL OF MATERIALS SCIENCE 26 (1991) 4631–4636

Effect of CeO_2 on reaction-sintered mullite–ZrO_2 ceramics

JENN-MING WU, CHICH-MAO LIN
Department of Materials Science and Engineering, National Tsing Hua University, Hsinchu, 30043 Taiwan

The effect of ceria on mullite formation and the sintering of zircon and alumina powders was investigated. Quantitative X-ray powder analysis was used to determine the formation of mullite and zirconia of both monoclinic and tetragonal forms. Scanning electron microscopy and electron-probe microanalysis were used for microstructural analysis. It was found that the addition of CeO_2 enhanced the formation of mullite and increased the fraction of tetragonal zirconia. The addition of CeO_2 caused the formation of mullite directly from reaction of zircon with alumina without decomposition of zircon into zirconia and silica. In addition to forming a liquid phase, the ceria essentially formed a solid solution with zirconia. The fracture toughness of the mullite–zirconia composites was about 5.5–6.0 MPa $m^{1/2}$.

1. Introduction

Mullite ceramics possess low thermal expansion, good high-temperature strength and creep resistance, and excellent stability suitable for high-temperature applications. However, as structural materials, the fracture toughness of mullite is only 1.8–2.8 MPa $m^{1/2}$ [1, 2]. To improve the toughness, a mullite–ZrO_2 composite is usually adopted. The production of mullite–ZrO_2 composite is mainly by two routes: the first one is to prepare mullite powder first, then mix with ZrO_2 and sinter at high temperature; the second one is to reaction-sinter $ZrSiO_4$ with Al_2O_3. The first method requires a high sintering temperature, generally higher than 1600 °C [3]. The second method can be performed at lower temperatures but temperatures higher than 1500 °C are still necessary [5–7]. Additives which enhance the reaction-sintering of the $ZrSiO_4$ and Al_2O_3 have been studied [8–10] and it was found that CaO, MgO and TiO_2 increased the formation of mullite and increased the toughness to 2.58–4.60 MPa $m^{1/2}$, depending on the nature and content of the additive. Thus, it was confirmed that suitable additives can help the reaction-sintering of $ZrSiO_4$ with Al_2O_3. In studies of ZrO_2-toughened ceramics, it was found that CeO_2 greatly increased the fracture toughness of ZrO_2 ceramics [11]. It is interesting to investigate the effect of CeO_2 as an additive in the reaction-sintering of the mullite–ZrO_2 composite.

2. Experimental procedure

CeO_2 not only dissolves in ZrO_2 but also reacts with Al_2O_3 and SiO_2. However, there is still no CeO_2–ZrO_2–Al_2O_3–SiO_2 phase diagram available, so the doping of CeO_2 was added as [8]

$$(2 + 2x)ZrSiO_4 + 3Al_2O_3 + x(CeO_2 + Al_2O_3)$$

where $x = 0.37$ and 0.60. The equivalent molar ratio is expressed in Table I. For $x = 0.37$, the CeO_2/ZrO_2 ratio locates in the tetragonal solid-solution region of the ZrO_2–CeO_2 phase diagram [12]; while for $x = 0.60$, the ratio falls in the mixture region of tetragonal and cubic solid solution. The raw materials were reagent-grade powders of $ZrSiO_4$, Al_2O_3, and CeO_2. The powders were weighed and milled in Al_2O_3 jars with Al_2O_3 balls in deionized water for 4 h. In addition, 1 wt % of polyvinyl alcohol was added in the mill as a binder. After milling, the suspension was dried with an infrared lamp and granulated by passing through a 100 mesh sieve. The powder was dry-pressed at 100 MPa to form discs of 1 cm diameter and 2.5 mm thickness. The pressed discs were then sintered at 1400, 1450 and 1500 °C for various durations of time.

After sintering, the bulk densities were measured by the Archimedes method; the average value of at least three samples is reported. The reaction products were identified by X-ray powder diffractometry (Rigaku). For qualitative analysis, the scanning speed was chosen as 2° min^{-1}, while for quantitative analysis of mullite and ZrO_2, a step scan was employed around the (1 1 1), (1 1 $\bar{1}$) peaks of monoclinic ZrO_2, the (1 1 1) peak of tetragonal ZrO_2, the (1 1 3) peak of α-Al_2O_3, and the (1 1 0) peak of mullite. Each step increment was 0.008° with 4 s dwell time. The equations [8, 13] used in the quantitative analysis are

$$W_M = \left[1 + \frac{1}{k}\left(\frac{I_{(1\,1\,3)A}}{I_{(1\,1\,0)M}}\right)\right]^{-1}$$

$$W_t = \frac{I_{1\,1\,1(t)}}{I_{1\,1\,1(t)} + I_{1\,1\,1(m)} + I_{1\,1\,\bar{1}(m)}}$$

where W_M and W_t express the content of mullite and the fraction of tetragonal ZrO_2, respectively. The I

0022–2461/91 $03.00 + .12

TABLE I The compositions investigated in the present study

	X = 0.37	x = 0.60
ZrO_2	29.7%	30.2
SiO_2	29.7	30.2
Al_2O_3	36.6	34.0
CeO_2	5.0	5.6
Total	100.0	100.0
CeO_2/ZrO_2	0.169	0.185

values are the integrated intensities of the above-mentioned peaks of the related phases; k is a constant which can be obtained by preparing known mixtures of ZrO_2, SiO_2, Al_2O_3 and mullite and obtaining a calibration curve. The k obtained this way is 0.58.

For microstructural observations, samples were polished and thermally etched at 1250 °C for 2 h and then investigated by scanning electron microscopy (SEM). For elemental analysis, electron-probe micro-analysis (EMPA) was used.

To determine the toughness, K_{IC}, a Vickers micro-hardness tester was used. The applied load was 20 kg. The formula of Evans and Charles [14] was used to calculate the K_{IC} values. Each K_{IC} value is the average of about 10 points. For flexural strength measurements, three-point bending of specimens of 38 mm $\times$ 4.4 mm $\times$ 2.6 mm was performed. The strain rate was 0.1 mm min^{-1}. For each modulus of rupture value, at least six specimens were tested.

3. Results and discussion

Fig. 1 shows the X-ray diffraction patterns of several powders containing different compositions. It illustrates that pure $ZrSiO_4$ with no additive remained unchanged after heating at 1400 °C for 2 h. On the other hand, $ZrSiO_4$ decomposed to ZrO_2 (mostly monoclinic) and SiO_2 after the same heating if Al_2O_3 was incorporated. However, no mullite was observed in this powder. This observation is similar to those of Claussen and Jahn [15]. Even though the reaction temperature was raised to 1500 °C, mullite was still not found in powders containing $ZrSiO_4$ and Al_2O_3. In contrast, the addition of CeO_2 into the powder containing $ZrSiO_4$ and Al_2O_3 changed the reaction in several ways. Fig. 1 shows that the decomposition of $ZrSiO_4$ was slowed down, and the transformation does not produce ZrO_2 and SiO_2 simultaneously. After reaction at 1400 °C for 2 h, most of the $ZrSiO_4$ remained unchanged, only some decomposed to ZrO_2 but no SiO_2 phase was observed. No formation of mullite was observed by X-ray diffraction analysis under these conditions. As the temperature was raised to 1450 °C, mullite was observed coexisting with ZrO_2 and $ZrSiO_4$ but still no SiO_2 phase was observed. A comparison of the results of 1400 and 1450 °C reaction shows that the addition of CeO_2 enhances the reaction of $ZrSiO_4$ directly with Al_2O_3 to form mullite and slows down the decomposition of $ZrSiO_4$ to ZrO_2 and SiO_2.

The results of quantitative X-ray diffraction analysis are shown in Figs 2 and 3. Fig. 2 demonstrates

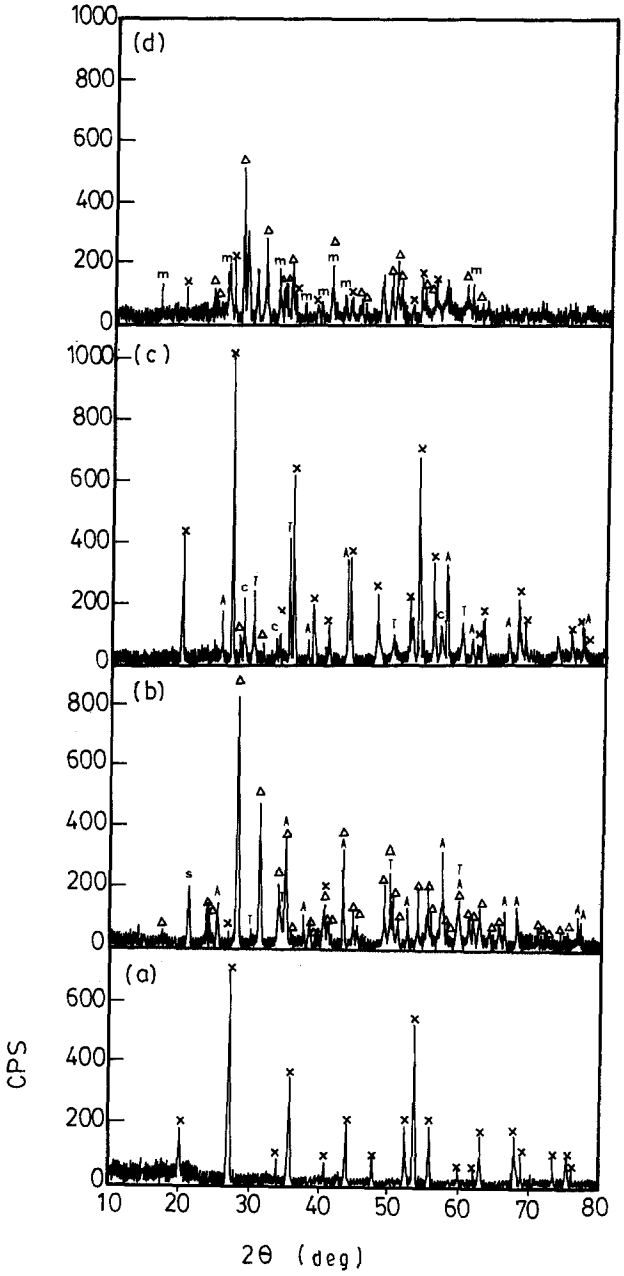

Figure 1 X-ray powder diffraction patterns of different powders and treatment conditions. (×) $ZrSiO_4$, (△) ZrO_2 (mono.), (T) ZrO_2 (tetra.), (m) mullite, (A) Al_2O_3, (c) CeO_2, (s) SiO_2.

that the amount of mullite increased with the amount of added CeO_2 and with temperature. The higher the temperature and the higher the CeO_2 content, the faster the amount of mullite reaches a saturation value which also increased with temperature and CeO_2 content. Fig. 3 shows that the tetragonal phase of ZrO_2 increases with the content of added CeO_2. Without addition of CeO_2, the ZrO_2 phase was almost all monoclinic at temperatures higher than 1450 °C, and only about 2% of ZrO_2 was tetragonal at 1400 °C 2 h reaction. The fraction of ZrO_2 generally decreased with reaction-sintering temperature and time duration.

Fig. 4a shows the polished and thermally etched surface of the composition $x = 0.37$ which was sintered at 1450 °C for 2 h. Fig. 4b–d shows the Al, Zr and Si mapping (EPMA) of Fig. 4a. From these photographs, it is seen that the large and darker grains

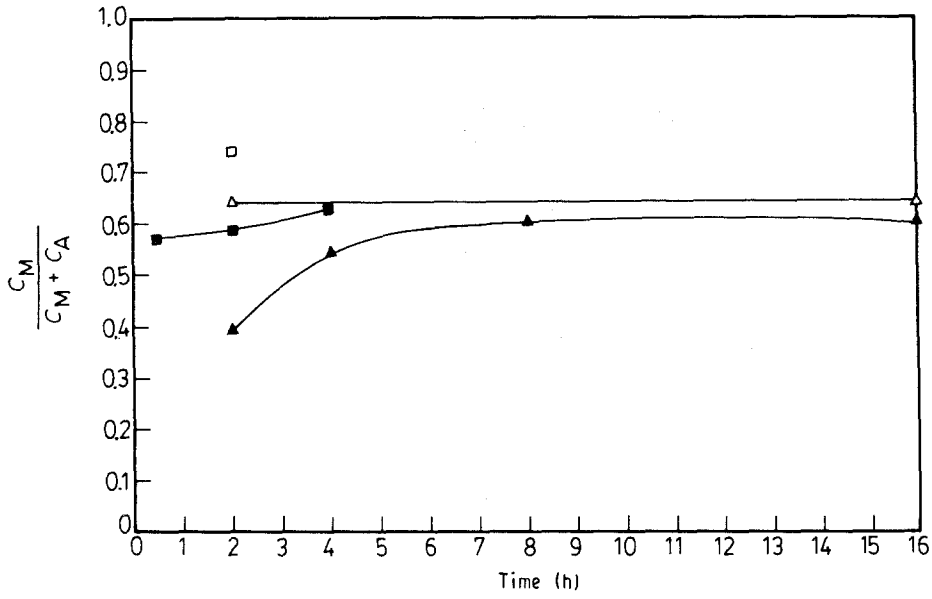

Figure 2 The fraction of mullite as calculated from quantitative X-ray diffraction analysis. CeO_2 $x = 0.37$: (▲) 1450 °C, (■) 1500 °C. $x = 0.60$: (△) 1450 °C, (□) 1500 °C.

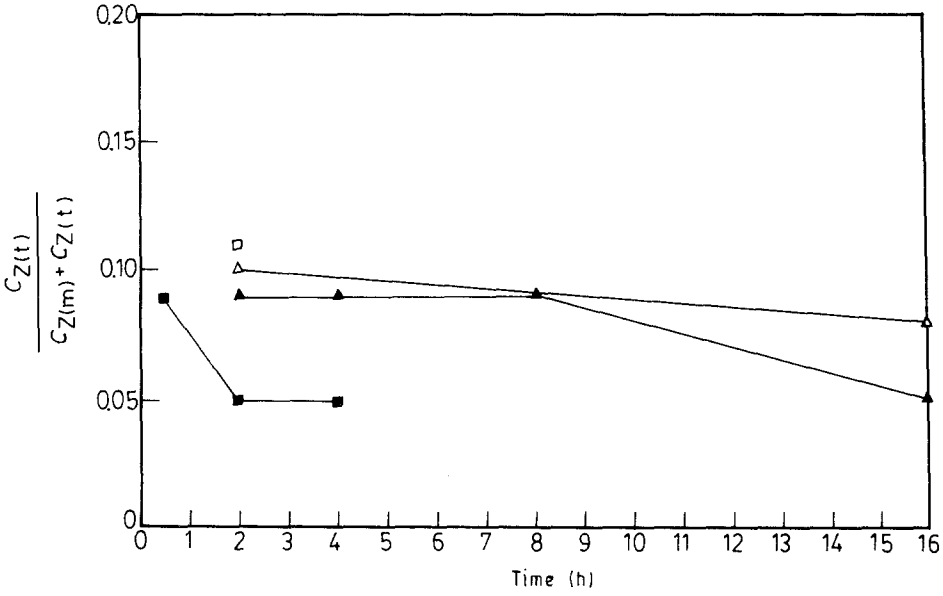

Figure 3 The fraction of tetragonal zirconia as calculated from quantitative X-ray diffraction analysis. CeO_2 $x = 0.37$: (▲) 1450 °C, (■) 1500 °C. $x = 0.60$: (△) 1450 °C, (□) 1500 °C.

(centre and left) are Al_2O_3, while the small and brighter grains containing Zr and Si are $ZrSiO_4$. Around an Al_2O_3 grain, especially at the left side of the central grain, there exists Si and an Al-rich and Zr-deficient area. This should be the newly formed mullite. The formation of mullite directly from $ZrSiO_4$ and Al_2O_3 is confirmed by Fig. 4.

Fig. 5 illustrates the polished and thermally etched surface of a well-reacted sample of $x = 0.37$ which was sintered at 1450 °C for 16 h. From X-ray powder diffraction analysis, this sample contains only ZrO_2, Al_2O_3 and mullite. The matrix is mullite and the bright grains are ZrO_2 which can be classified as intergranular and intragranular. The intergranular ZrO_2 is located around the edge of the matrix phase with a grain size of about 2–5 μm, while the intragranular ZrO_2 is located in the matrix with a size of about 0.5–1 μm. In addition, there are dark grains in the matrix which are Al_2O_3. The average grain size of ZrO_2 increases with sintering temperature and time duration, which should be responsible for the reduced fraction of tetragonal ZrO_2. Fig. 6 shows X-ray line profiles of Ce and Zr of a polished surface, illustrating that most of the Ce dissolves in Zr. The dissolution of Ce in ZrO_2 explains the increase of tetragonal ZrO_2 content.

In addition to the above-mentioned observations, it was found that there were some liquid-like phases formed on the surface of the ceramics with CeO_2 dopants when the ceramics were sintered at temperatures higher than 1450 °C. The constituents of the liquid-like phase were determined by EPMA point analysis to be Al, Si and Ce.

Fig. 7 shows the sintered density of ceramics doped with $x = 0.37CeO_2$. The sintered density at 1400 °C increases with time initially and decreases in the later

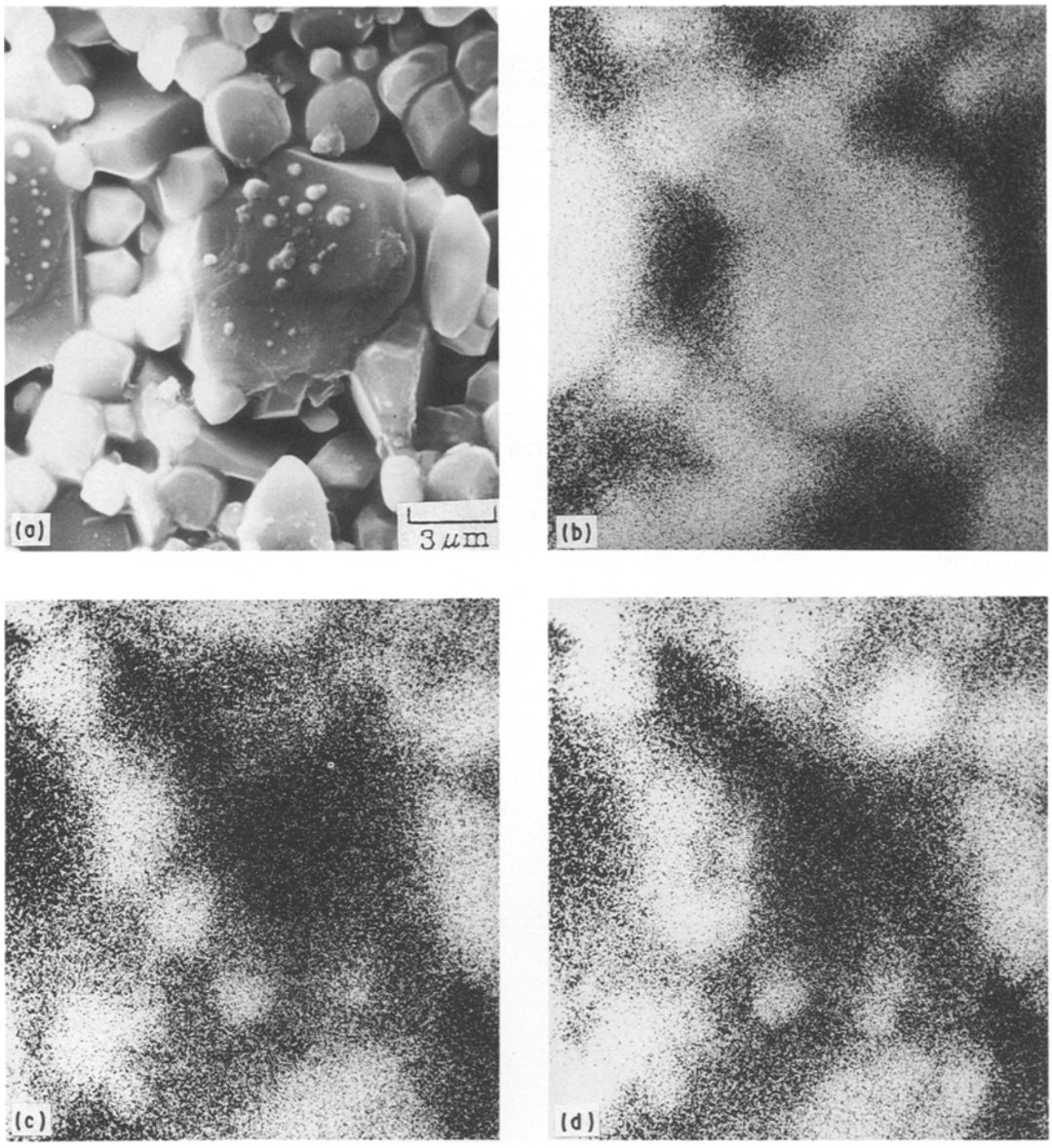

Figure 4 Microstructures of initially reacted zircon–alumina–ceria ceramics: (a) SEM, (b) Al, (c) Zr and (d) Si.

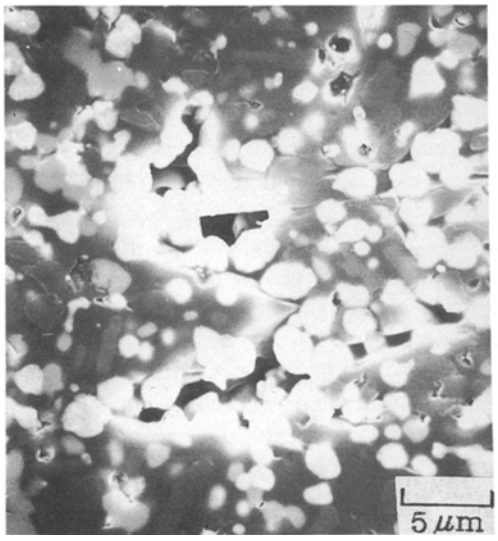

Figure 5 Microstructures of well-reacted zircon–alumina–ceria ceramics.

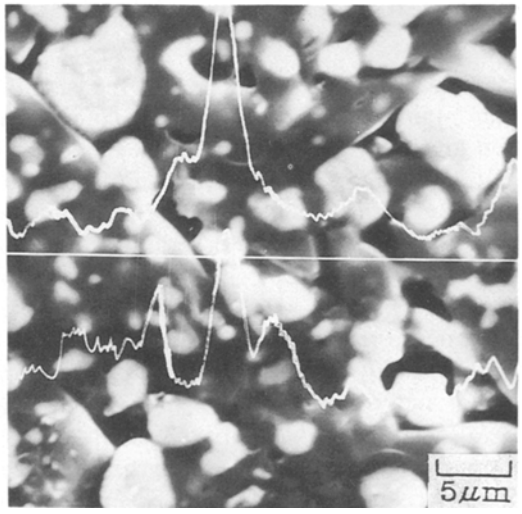

Figure 6 X-ray line profiles of Ce (above) and Zr (below) obtained from EPMA.

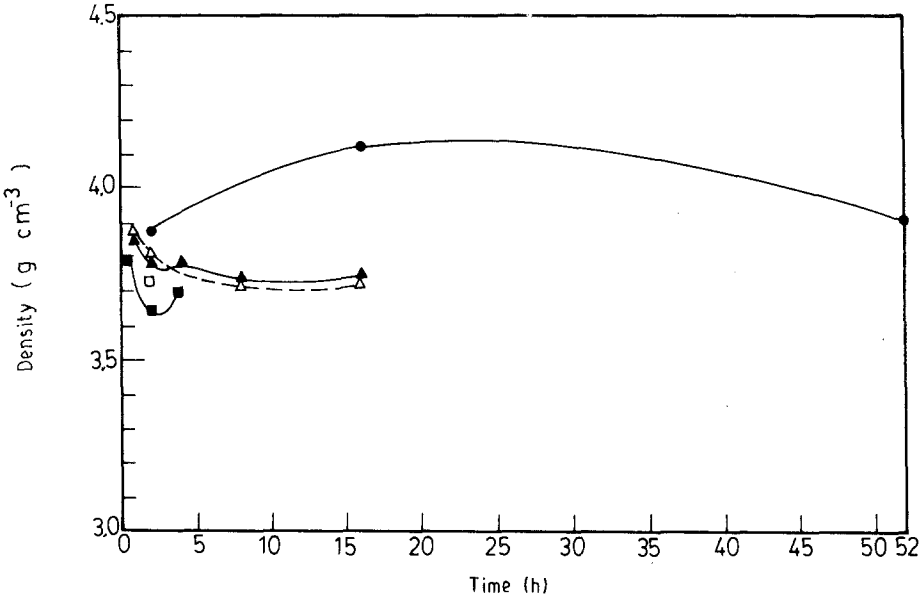

Figure 7 Sintered density versus sintering time for $x = 0.37$ at 1400, 1450 and 1500 °C. CeO_2 $x = 0.37$: (●) 1400 °C, (▲) 1450 °C, (■) 1500 °C. $x = 0.60$: (△) 1450 °C, (□) 1500 °C.

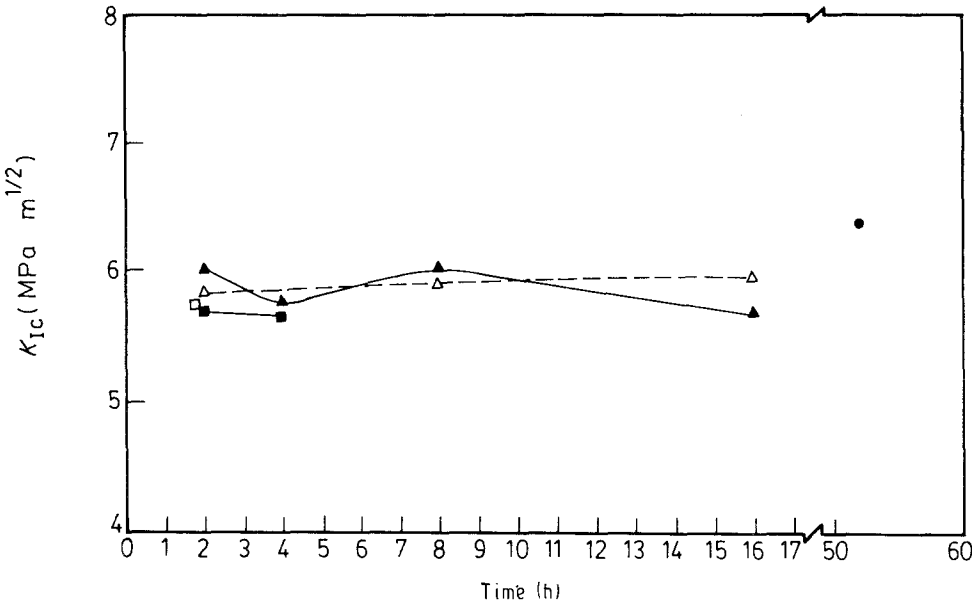

Figure 8 Fracture toughness of reaction-sintered mullite–ZrO_2 ceramics. CeO_2 $x = 0.37$: (●) 1400 °C, (▲) 1450 °C, (■) 1500 °C. $x = 0.60$: (△) 1450 °C, (□) 1500 °C.

stage. At 1450 °C, the sintered density was observed to decrease with sintering time from the start of sintering. In contrast, the sintered density at 1500 °C decreased with time in the beginning and then reversed to an increase with time. The sintered densities of ceramics doped with $x = 0.60CeO_2$ exhibited similar behaviour and will not be shown here.

The sintering behaviour can be explained with the aid of the results of X-ray diffraction analysis. The possible reasons for a reduction of density are: first, an increase of porosity; and/or, second, a reduction of the density of the reaction product. To determine the true reason for this density reduction with time, the ceramics were polished and then investigated with SEM to calculate the porosity by quantitative microstructural analysis. The porosities obtained are 10.8 and 4.5 vol % for $x = 0.37$ and sintering at 1450 °C for 2 and 16 h, respectively; and they are 4.9 and 4 vol % for $x = 0.37$ and sintering at 1500 °C for 2 and 4 h, respectively. The situation is similar for the composition doped with $x = 0.60CeO_2$, but with lower porosity. This rules out the possibility of density reduction due to an increase of porosity.

The densification proceeds during the whole sintering period. The densities of reaction products are 4.68 g cm^{-3} for $ZrSiO_4$, 6.10 g cm^{-3} for ZrO_2 (tetragonal), and 5.83 g cm^{-3} for ZrO_2 (monoclinic); while it is only 3.70 g cm^{-3} for the mullite phase. Therefore, the sintered density would decrease with the increasing amount of mullite formed. The formation of mullite is very slow at 1400 °C for $x = 0.37$, and thus the density decreases only after sintering for longer than 16 h. At 1450 °C the formation of mullite increases with time, which causes the density reduction from the

beginning of sintering. For 1500 °C, the reaction rate of mullite is even faster so that the mullite reaches a saturated value in a much shorter time. The density increases with time due to densification after the mullite content reaches a saturation value.

Fig. 8 shows the K_{IC} values of the sintered ceramics. The K_{IC} values shown in the figure are the average values from about ten measurements each. The determined K_{IC} values are about 5.5–6 MPa $m^{1/2}$, significantly higher than that of mullite, ~ 2 MPa $m^{1/2}$. There is no direct relationship between the K_{IC} value and the content of ZrO_2 (tetragonal). The modulus of rupture values are determined to be about 125 MPa for all ceramics doped with CeO_2 with $x = 0.37$ or 0.60 and sintered at 1450 °C for 16 h or 1500 °C for 2 h. The relatively low MOR values compared with previous studies [8–10] may be due to the non-uniform characteristics of the sintered ceramics. More advanced powder preparation techniques would improve the properties and thus deserve further studies.

4. Conclusion

The formation of mullite is enhanced by the addition of CeO_2 to the $ZrSiO_4$–Al_2O_3 powder compacts. The addition of CeO_2 causes the formation of mullite directly from the reaction of $ZrSiO_4$ with Al_2O_3 and suppresses the decomposition of $ZrSiO_4$ into ZrO_2 and SiO_2. The content of the reacted mullite and the fraction of the tetragonal ZrO_2 increase with the amount of CeO_2. The CeO_2 essentially forms a solid solution with ZrO_2. In addition, the addition of CeO_2 also forms some liquid phase with Al_2O_3 and SiO_2. The addition of CeO_2 has the effect of increasing the fracture toughness: K_{IC} increases to about 5.5–6 MPa $m^{1/2}$, higher than that of mullite.

References

1. TAI-IL MAH and K. C. MAZDIYASNI, *J. Amer. Ceram. Soc.* **66** (1983) 699.
2. S. KANZAKI, H. TABATA, T. KUMAZAWA and S. OHTA, *ibid.* **68** (1985) C6.
3. QI-MING YUAN, JIA-QI TAN and ZHENG-GUO JIN, *ibid.* **69** (1986) 265.
4. J. S. MOYA and M. I. OSENDI, *J. Mater. Sci.* **19** (1984) 2909.
5. P. BOCH and J. P. GIRY, *Mater. Sci. Eng.* **71** (1985) 39.
6. G. ORANGE, G. FANTOZZI, F. CAMBIER, C. LEBLUD, M. R. ANSEAU and A. LERICHE, *J. Mater. Sci.* **20** (1985) 2533.
7. F. CAMBIER, C. BAUDIN de La LASTRA, P. PILATE and A. LERICHE, *Brit. Ceram. Trans. J.* **83** (1984) 196.
8. P. PENA, P. MIRANZO, J. S. MOYA and S. de AZA, *J. Mater. Sci.* **20** (1985) 2011.
9. P. MIRANZO, P. PENA, J. S. MOYA and S. de AZA, *ibid.* **20** (1985) 2702.
10. M. F. MELO, J. S. MOYA, P. PENA and S. de AZA, *ibid.* **20** (1985) 2711.
11. J. G. DUH, H. T. DAI and B. S. CHIOU, *J. Amer. Ceram. Soc.* **71** (1988) 813.
12. P. DUWEZ and F. ODELL, *ibid.* **30** (1950) 280.
13. R. C. GARVIE and P. S. NICHOLSON, *ibid.* **55** (1972) 303.
14. A. G. EVANS and E. A. CHARLES, *ibid.* **59** (1976) 371.
15. N. CLAUSSEN and J. JAHN, *ibid.* **63** (1980) 224.

Received 25 April
and accepted 20 December 1990